© Universiti Tun Hussein Onn Malaysia Publisher's Office

IJIE

Journal homepage: http://penerbit.uthm.edu.my/ojs/index.php/ijie

ISSN : 2229-838X e-ISSN : 2600-7916

The International Journal of Integrated Engineering

Utilizing Artificial Neural Network and Multiple Linear Regression to Model the Compressive Strength of Recycled Geopolymer Concrete

Stephen Adeyemi Alabi[1*], Jeffrey Mahachi[1]

[1]Department of Civil Engineering Technology, University of Johannesburg, Doornfontein Campus, Johannesburg, 2028 SOUTH AFRICA

*Corresponding Author

DOI: https://doi.org/10.30880/ijie.2022.14.04.005

Received 4 July 2020; Accepted 31 August 2021; Available online 20 June 2022

Abstract: Based on the heterogeneity of concrete constituents as well as variability in compressive strength over many magnitudes for various types of concrete, predictive methods for evaluating the compressive strength have now been given considerable attention. As a result, this research compares the performance of the Artificial Neural Network, ANN, in forecasting the compressive strength of geopolymer recycled concrete (GPRC) based on selected pozzolans (Coal Fly Ash (CFA) and Rice Husk Ash (RHA)) at ages 7, 28, and 56 days to the traditional Multiple Linear Regression, MLR. The compressive strength of GPRC-based CFA and RHA was determined using 65 concrete samples from eight different mixtures. The developed models were based on the experimental results, which used varying material quantities. The ANN and MLR models were built with eight input variables: Ordinary Portland cement (OPC), RHA, CFA, Crushed granite (CG), Cupola Furnace Slag (CFS), Alkaline Solution (AS), Water-Binder Ratio (WB), and Concrete Age (CA), with compressive strength being the only predicted variable. Using MATLAB® code, approximately 75% and 25% of the input data were used for training and testing to develop an ANN model for predicting compressive strength, f_{cu}. For ANN and MLR, the input data were trained and tested using the feedforward back-proportion and backward elimination approaches, respectively. Based on satisfactory performance in terms of means square error MSE, the most likely model architecture containing eight input layers, thirteen hidden layers, and one output layer neurons was chosen after several trials. According to the MLR results, only three input variables, CFA, CG, and CA, are statistically significant with *p*-values less than 0.05. R^2 = 0.9972, MSE = 0.4177, RMSE = 1.8201, for ANN and R^2 = 0.7410, MSE = 66.6308, RMSE = 290.4370, for MLR. The predicted results demonstrate the proposed model's dependability and computational forecasting capability. The findings of the study have the potential to help a wide range of construction industry in predicting the concrete properties and managing scarce resources.

Keywords: Artificial Neural Network, Multiple Linear Regression, Geopolymer concrete, compressive strength, cupola furnace slag, rice husk ash

1. Introduction

Concrete is well-known as one of the main building materials for long-term human settlements. Various types of waste from the population, agriculture, and industrialization have been shown in studies to substitute for conventional materials in concrete. As sustainable and eco-friendly materials, these types of waste have contributed significantly to the principles of sustainability in the built environment. Numerous studies have been conducted to investigate the possibility of reducing, recycling, and reusing wastes such as cupola furnace slag (CFS) [1]-[3], coal fly ash (CFA) [4]-[6], and rice husk ash (RHA) [7]-[8] for concrete production. However, recycled aggregate concrete [9]-[13], self-compacting concrete [14]-[16], and geopolymer concrete (GPC) [17]-[24] have all been made from these waste materials. These studies revealed the possibility of using these waste materials as long-term substitutes for

*Corresponding author: aalabi@uj.ac.za

traditional building materials like cement and aggregates.

As a result, despite numerous studies on the GPC, its use as a construction material remains limited. This could be because there is currently no standard mix design or sufficient data to predict its performance. Due to the complex and imprecise physical processes involved in its production, GPC exhibits a wide range of uncertain behavior. As a result, it may result in resource waste, which may contribute to environmental pollution. To avoid repeating experiments and wasting scarce resources, simple models based on regression best fit curve have emerged, capable of reproducing the properties of concrete [25]-[29]. Because of the nonlinear behavior of concrete and the uncertainties associated with its production, these methods cannot adequately predict its correct behavior.

Surprisingly, applications of Artificial Neural Networks (ANNs) have been discovered to model any nominated material properties based on the given input parameters. Furthermore, ANN has grown in popularity and demonstrated some success in modeling concrete properties. [25] [26] [30]-[40]. ANNs can model any complex problem with a nonlinear relationship between the model parameters and engineering knowledge about the material's (e.g., concrete's) properties. MLR analysis, another modeling approach, models the relationship between a response/prediction parameter and a collection of independent parameters. It is an extension of the linear regression model [41-43]. As a result, this research focuses on the performance of ANN and MLR techniques for modeling and estimating compressive strength, f_{cu} of GPC. The methods were also trained, validated, and evaluated in terms of performance.

2. Materials and Methods

2.1 Experimental Setup and Results

Smooth surface granite with sizes ranging from 10 mm to 19 mm was used as a coarse aggregate. The cupola furnace slag (CFS) used as coarse aggregate was obtained in large quantities from the foundry dumpsite [1][7]. CFS was stored for an extended period to reduce the absorption effect caused by free oxides, primarily to control swelling. It was then pulverized into particles ranging in size from 10 mm to 19 mm. As a fine aggregate, well-graded river sand (RS) was used. The maximum grain size of RS that could be used was 4.75 mm. The cement used was 3X ordinary Portland cement (OPC) of grade 42.5, as specified by BS 12 [44]. This study used rice husk (RH) and coal fly ash (CFA) as geopolymer binders. For mixing, binding, and curing concrete samples, portable water conforming to ASTM 1602 [45] was used.

CFA and RHA were used as cement substitutes. Likewise, CFS was used to replace granite. The RS proportion was held constant at 100%, and the water-binder ratios were 0.50 and 0.64, respectively. Table 1 shows the input and predicted data used in ANN and MLR modeling for training and testing. For all concrete constituents, the maximum and minimum bounds were defined as 0% and 100%, respectively, in this study. As an alkaline solution, a mixture of NaOH and Na_2SiO_3 was used. The NaOH/Na_2SiO_3 ratio was 1:2.5. Concrete cubes with dimensions of 150 x 150 x 150 mm were made using a mix ratio of 1:2:4 by weight of binders, fine and coarse aggregates, and various water-binder ratios. After 24 hours of casting, the hardened samples were removed from the mold and cured in a water tank. The concrete cubes were crushed after 7, 14, 28, and 56-d curing periods.

Table 1 - Input and output data for ANN and MLR modelling

Input	Minimum	Maximum
OPC (%)	0	100
RHA (%)	0	25
CFA (%)	0	20
CG (%)	0	100
CFS (%)	0	35
Alkaline solution ratio (AS), (%)	0	0.4
Water-binder ratio (WB), (%)	0.50	0.65
Concrete age (CA), (days)	7	56
Output		
Compressive strength, f_{cu}, N/mm^2		

2.2 Artificial Neural Network Architecture

Because of its versatility in solving multidimensional or unidentifiable problems and being the most prevalent network architecture, the Multilayer Perception Levenberg-Marquardt (MLP) principles with feedforward back-proportion model were adopted [46][47]. In addition, Zuruda [48] discovered that the back-propagation training algorithm produces the best compressive strength prediction model compared to other training algorithms. The network is made up of nodes, which are also known as neurons. The neurons are divided into three primary nodal layers: input, hidden, and output. However, the input layer is not usually considered a neuron because it does not process any signals. Each node, however, was linked to all of the nodes in the adjacent layers. The network received the scaled data at nodes in the input layer and distributed it via the hidden transitional layer to the output layer. Weightings are applied to each connection/node to change the signal strength.

The MLP feeds the ANN the training dataset and modifies the weights to reduce or minimize the error function between the observed and desired outputs. In other words, a neuron's output is the weighted sum of its inputs plus the bias activated by the transfer function, as shown in Equation (1).

$$O = f(\varphi) = f\left(\sum_{i=1}^{n} w_i x_i + b\right) \tag{1}$$

where O is the output (response variable), x_1, $x_2,\ldots,x_n$ are the inputs, w_i is the weight vector, b is a bias, and the function $f(\varphi)$ is known as an activation function. The variable φ is defined as a scalar product of the weight and input vectors in Equation (2).

$$\varphi = w^T x = w_1 x_1 + w_2 x_2 + \ldots + w_n x_n \tag{2}$$

where T is the transpose of a matrix.

Typical modeling of a multilayered neural network is shown in Figure 1. The signal movement from inputs x_1, $x_2,\ldots,x_n$ is regarded as one-way, indicated by arrows, as a neuron's output signal flow (O).

In this study, 75% of the input data was used for training to create an ANN model for predicting compressive strength, f_{cu}, with MATLAB® code. The eight input variables used for neural network training are OPC, RHA, CFA, CG, CFS, AS, WB, and CA. In other words, there are eight neurons in the input layer. Because f_{cu} is the only output, the output layer has only one neuron. Because there is no universal method for defining the number of neurons in each hidden layer. Before determining the most likely number of hidden layers and neurons that met the Mean Square Error, MSE criteria, many trials were conducted. Following that, the network was ready for validation. In other words, after completing the training process, the network was given testing data to validate and evaluate the trained network's integrity. System error is defined as the difference between observed and predicted (output) values in this study. During ANN training, the network error is minimized by changing the weight, and thus the number of nodes in the hidden layer is determined by a series of network trial and error methods.

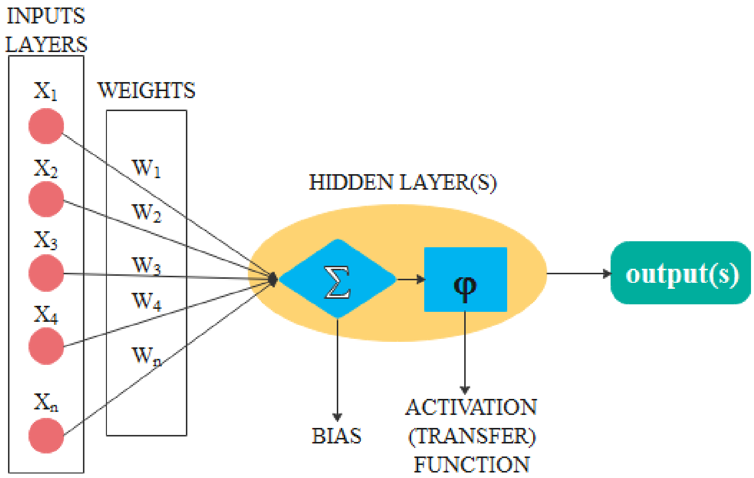

Fig. 1 - Architecture of an artificial neuron and a multilayered neural network

2.3 Multiple Linear Regression Model (MLR)

Many engineering problems require the interaction of two or more parameters. As a result, MLR is one of the most powerful tools for predicting the most likely relationship between response and many independent parameters. In other words, MLR modeling seeks to evaluate a statistical function that connects the input parameters to the output model parameters using several independent estimations. Regression modeling assumes that a linear combination of input data can describe the predicted outcome. As a result, the MLR model was created by using 75% of the dataset for training and the remaining 25% to test the model's performance. SPSS Software version 21 was used to run the MLR model for compressive strength, f_{cu}, prediction. The general form of the MLR equation is shown in Equation 3:

$$y = \beta + \alpha_1 x_1 + \alpha_2 x_2 + \alpha_3 x_3 + \ldots + \alpha_n x_n \tag{3}$$

where y is the predicted model parameter representing compressive strength, f_{cu}, β is the intercept, $\alpha_1, \alpha_2, \alpha_3, \ldots, \alpha_n$ are regression coefficients, and x_1, x_2, $x_3, \ldots, x_n$ are independent parameters referring to basic concrete properties (i.e., the input data).

The hypothetical collinear relationship between independent parameters is one of the MLR properties. The variation inflation factor (VIF) is an indicator used to determine collinearity. If there is no linear correlation between the independent parameters, the VIF value is unity, and any variation from unity indicates the possibility of collinearity. Having more than ten as VIF values for each parameter implies multiple collinearities, leading to computational or estimation errors.

2.4 Performance Appraisal

The performance appraisal of the developed ANN and MLR models was determined using the following major statistical indices, which were deemed significant: mean squared error (MSE), the root of the mean squared error (RMSE), and multiple coefficients of determination (R^2), as shown in Equations 4, 5, and 6.

$$MSE = \frac{1}{N_d} \sum_{i=1}^{n} \left(\hat{O}_i - O_i \right)^2 \tag{4}$$

$$RMSE = \sqrt{\frac{1}{N_d} \sum_{i=1}^{n} \left(\hat{O}_i - O_i \right)^2} \tag{5}$$

$$R^2 = 1 - \frac{\sum \left(\hat{O} - O \right)^2}{\sum \left(\hat{O} - \bar{O} \right)^2} \tag{6}$$

where $\hat{O}$ is the observed value, O is the predicted value of $\hat{O}$, and $\bar{O}$ is the mean value of the $\hat{O}$ values. N_d is the total number of data.

R^2, as defined by equation 6, is the fraction of total variation in the predicted (response) parameter described by various independent parameters. R^2 increases as the difference between observed and predicted values decreases. R^2 is usually between 1 and 0. R^2 near 1 indicates how well the regression model fits the observed data, while R^2 near 0 indicates a poorly fit model.

3. Results and Discussion

3.1 Artificial Neural Network (ANN)

3.1.1 ANN Training

The ANN was trained for compressive strength, f_{cu} prediction using eight input parameters. To avoid strenuous training processes that result in convergence problems, it is recommended that data be normalized before training a neural network [53]. Using Equation 7, one of the simple data normalization methods available was the Min-max normalization approach, which was used to bring the data values between 1 and 0.

$$\hat{y}_i = \frac{\hat{O} - \hat{O}_{\min}}{\hat{O}_{\max} - \hat{O}_{\min}} \tag{7}$$

where $\hat{y}_i$, $\hat{O}$, $\hat{O}_{\max}$, and $\hat{O}_{\min}$ are the normalized, observed, maximum and minimum values.

As shown in Figure 2, the most likely ANN architecture that produced the best result after several network trainings contains one hidden layer with thirteen neurons (i.e., 8-13-1), with the lowest MSE value compared to other trials.

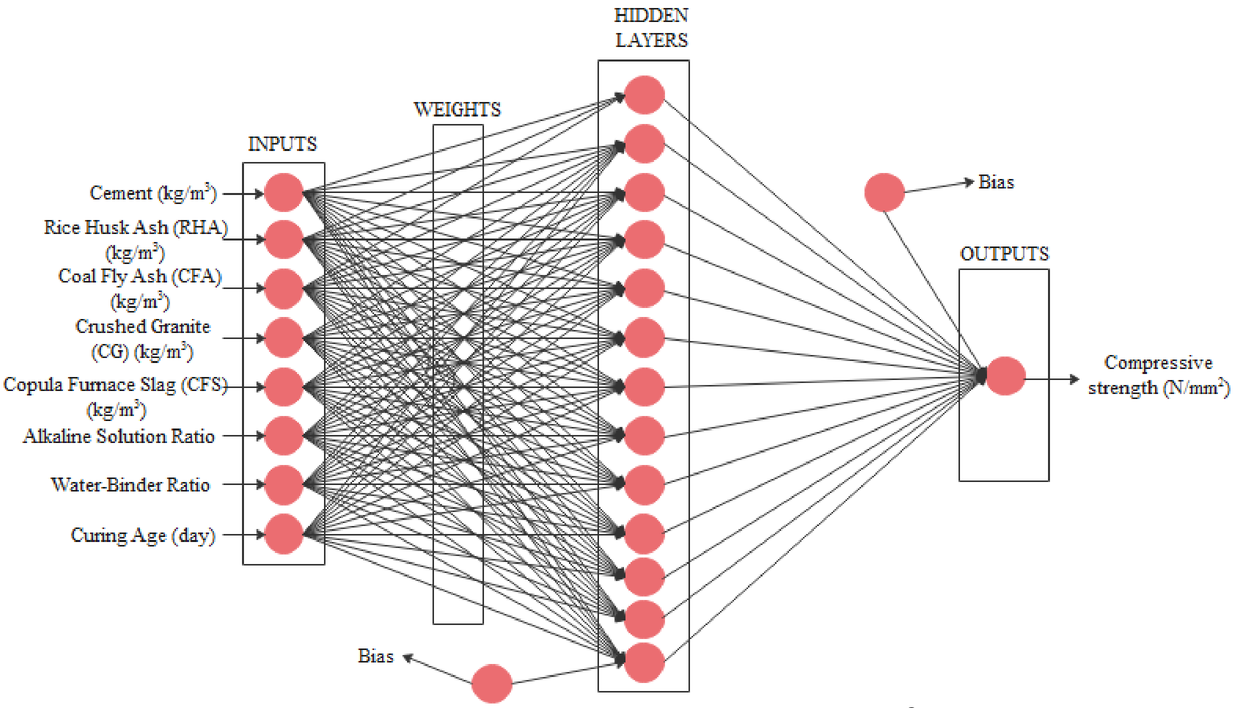

Fig. 2 - Optimum ANN architecture for compressive strength, N/mm^2 prediction

3.1.2 ANN Model Validation

The predicted values were calculated using the most likely ANN model among many ANN model classes (after several trials). Using compressive strength data sets, Figure 3 depicts the matching of observed and predicted data values and the corresponding error values. The matches are generally satisfactory. There was also found to be a strong statistical correlation between the predicted and observed data. This could be due to a minor discrepancy between the two sets of data. In other words, the most likely ANN prediction model was chosen was very close to the observed data, with a negligible phase shift. This means that, given the input parameters, the model can reproduce the experimental data with high prediction accuracy.

Likewise, the proposed ANN model could comprehend the relationship between various input and output parameters. The figure shows that the corresponding percent error values for the predicted f_{cu} are negligible, indicating a statistically reliable prediction model. As a result, the proposed ANN model class selected successfully predicts the f_{cu} based on the set of observed test data.

In addition, a new dataset was presented to the model to evaluate its performance and ability to generalize prediction beyond the training data. Figure 4 depicts the difference between the concrete samples' predicted and observed f_{cu} values for training and testing. The graph also confirms the existence of a strong correlation between experimental and predicted values. The ANN model's performance is estimated in Table 2. The calculated values for R^2, MSE, and RMSE, for test data are 0.9972, 0.4177, and 1.8201, indicating acceptable accuracy. Based on the calculated value of R^2, it implies that the eight (8) input variables explained 99.72 percent of the variation in compressive strength, f_{cu}, with the least amount of error, thereby validating the model. This may also imply that the chosen ANN model can predict the outcome of the measured data with a 95% confidence level.

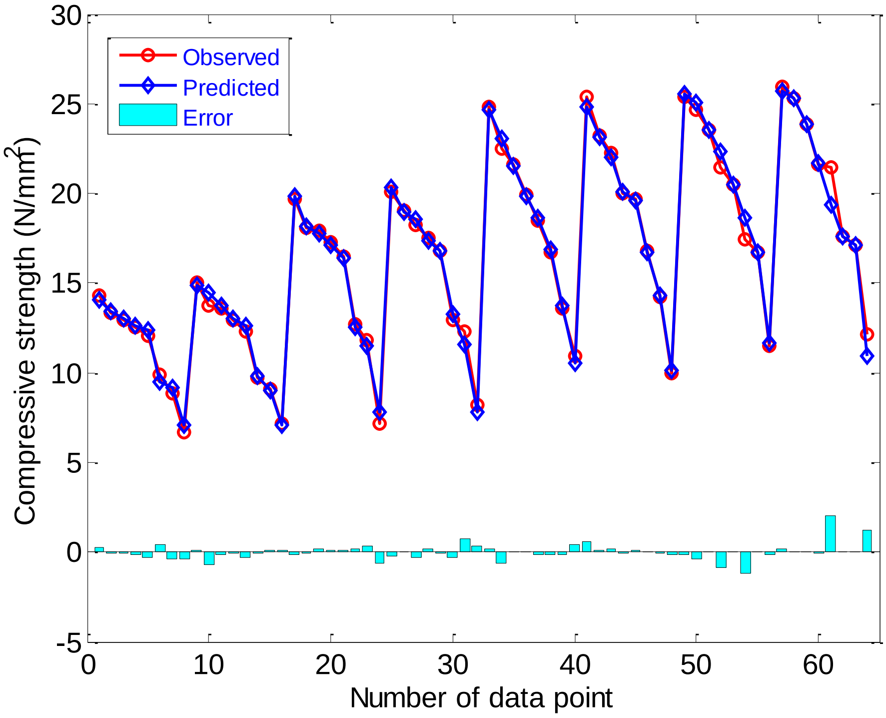

Figure 3 - Observed and predicted values of f_{cu} for all data

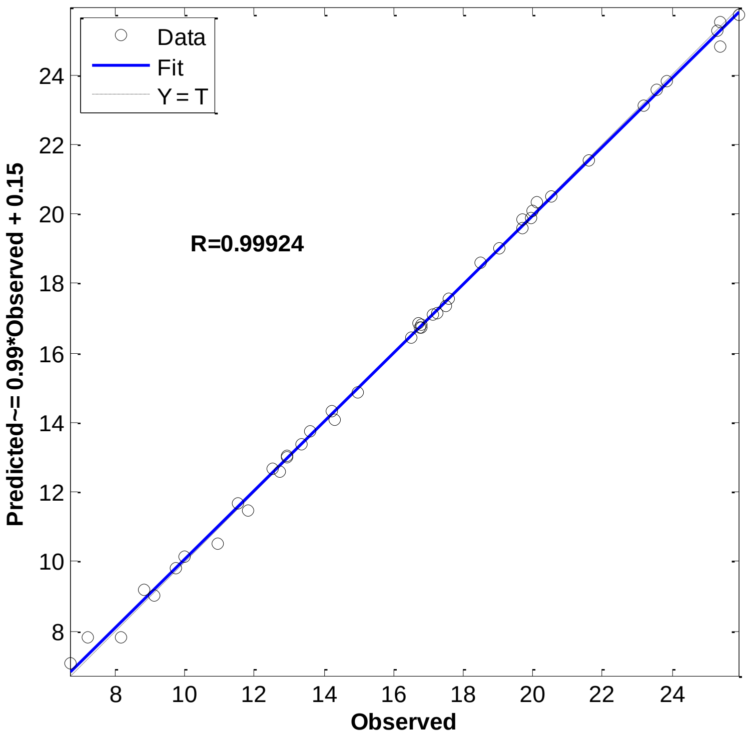

(a) Training data

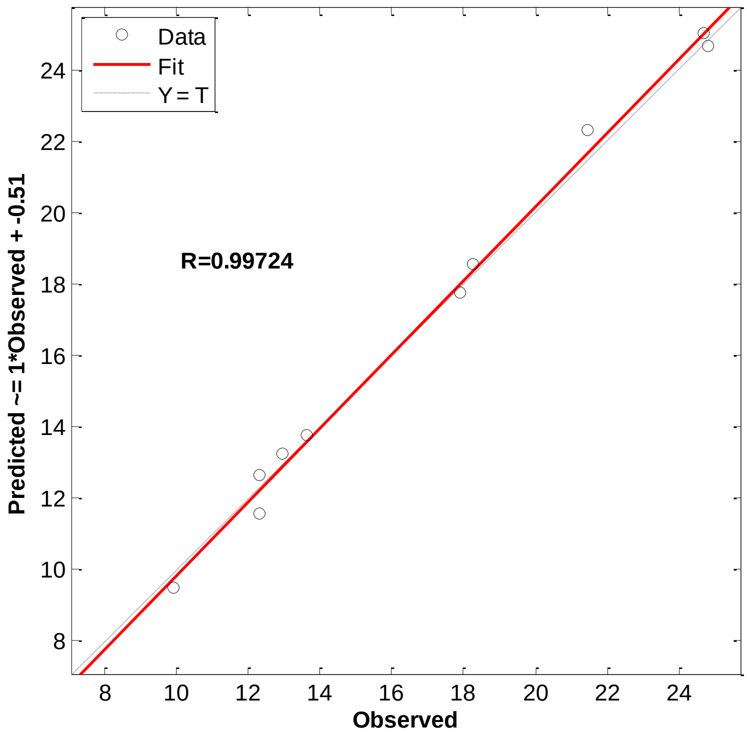

(b) Testing data

Figure 4 - Scatter plot of observed and predicted values of f_{cu} for most probable ANN model (a) training and (b) testing

Table 2 - Performance indices for optimum ANN model.

ANN	R^2	r	MSE	RMSE	MAPE
Training	0.9992	0.9996	0.0853	0.5724	0.7073
Testing	0.9972	0.9986	0.4177	1.8201	2.2935

3.2. Multiple Linear Regression (MLR) Model

3.2.1. Training of MLR Model

The MLR model for f_{cu} prediction was trained using 75% of the data as previously mentioned, with eight input variables. Table 3 summarizes the developed MLR model. The residual (error) values are the differences between the observed and predicted values of the fitted regression line. Residual values can be positive or negative; residuals greater than zero indicate that the proposed regression model predicted a too-small value than the observed value. Negative values indicate that the regression model predicted an incorrect value. As shown in Table 3, 'Min' represents the minimum residual value, 'Max' represents the maximum residual value, and 'Median' represents the median value. The median residual value of a good model is expected to be near zero, with the minimum and maximum values having nearly the same magnitude. The residuals for this model, as shown in the table, deviate slightly from these conditions. A graphical representation of the residual values can also be used to diagnose the model for normality and influential observations.

As a result, the residuals are expected to be distributed randomly in the vicinity of the horizontal line representing a residual error of zero. In other words, a good model's residual should be in the neighborhood, i.e., not too far away from the mean of zero. The residuals for the developed model, as shown in Figure 5, are not too far from the horizontal line of zero residual value and are roughly balanced except for a few points. Another plot to evaluate the distribution of residuals is the normal probability (or P-P) plot. The points for normally distributed residuals would be plotted to follow a straight line in the P-P plot. This model slightly diverges, indicating that the residual distribution is not entirely normal. Figure 5 shows that some of the predictors in the regression have little or no effect on predicting the f_{cu} or that the predictors chosen are insufficient to explain the data.

The coefficients of each independent (model parameters) variable are shown in the second column of Table 3. As a result, an MLR analysis was used to perform the performance analysis of input factors on f_{cu}, and the model is expressed in Equation (8).

$$f_{cu} = -11.828 - 0.051RHA + 0.076CFA + 0.291CG - 4.749WB + 0.352CA \quad (8)$$

The standard statistical error for each of the model parameter coefficients is shown in the third column of Table 3. The standard error for an acceptable model should be at least five to ten times smaller than the corresponding coefficient. The statistical standard errors produced by this model were nearly as large as the corresponding coefficients of each input variable. Coefficient's significance or *p*-value, present on fourth column of Table indicates the likelihood that the corresponding coefficient is not relevant in the model. The *p*-values revealed that CG and CA were the only statistically significant variables, while other variables were not statistically significant enough to establish significant models by MLR.

The MLR was re-trained using the backward elimination algorithm to determine which predictors should be used in developing the model and which should be discarded. Each predictor in the model had its *p*-value calculated. The predictor with the highest *p*-value is statistically insignificant. In contrast, the *p*-value equals 0.05 threshold is predetermined, below which the predictor has a greater than 95% chance of being meaningful. The predictor with a *p*-value greater than the threshold value is removed from the model and recalculated. With three (3) input variables, Regression Equation 9 was created. According to the model results in Tables 3 and 4, Equation 9 is more reliable than Equation 8. The three variables, CFA, CG, and CA, are statistically significant with *p*-values less than 0.05 and VIF close to 1.

$$f_{cu} = -21.224 + 0.138CFA + 0.357CG + 0.347CA \quad (9)$$

Table 3 - Summary of the parameter estimates, residual, standard errors for the linear compressive strength model, N/mm^2 fitted with 5 predictors

Input variables	Coefficients	Estimates Standard Error	*p*-valves	VIF
Constant	-11.828	14.330	0.414	-
RHA	-0.051	0.112	0.652	16.537
CFA	0.076	0.141	0.593	18.787
CG	0.291	0.139	0.043	49.228
WB	-4.749	3.019	0.124	1.021
CA	0.352	0.027	0.000	1.028
Residual	Min	Max	Median	Standard Deviation
	-3.3799	2.2780	0.0000	1.4121

Table 4 - The parameter estimates, residual, standard errors for the linear compressive strength, N/mm^2 model, fitted with 3 predictors

Input variables	Coefficients	Estimates Standard Error	*p*-valves	VIF
Constant	-21.224	3.840	0.000	-
CFA	0.138	0.064	0.037	3.835
CG	0.357	0.039	0.000	3.866
CA	0.347	0.027	0.000	1.016
Residual	Minimum	Maximum	Median	Standard Deviation
	-3.4925	2.2809	0.0000	1.4597

3.2.2 Verification of MLR Model

After determining the regression equations, the model equations were fitted to the test data to predict f_{cu}. Figures 6 and 7 show correlation plots for observed f_{cu} values versus expected values for the training and test datasets, respectively. The performance of the developed MLR models was evaluated using the obtained values of MSE, RMSE, and R^2 between measured and predicted values, as shown in Tables 5 and 6. Table 6 shows that R^2 and r for Equation 9 have better and more reliable performance than Equation 8 with 5 input variables. The three input variables (CFA, CG, and CA) explained 74.10% of the variation in f_{cu} for Equation 9.

In contrast, the five input variables explained 73.62% of the variation in f_{cu} for MLR, as presented in Equation 8. The correlation coefficient, r, for the MLR model (Equation 9) indicates a stronger linear relationship between the observed and predicted values of f_{cu} compared to the r-value for the MLR model in Equation 8. Because R^2 and r values can provide a skewed estimate of model performance, the MLR models are also compared in terms of MSE, RMSE, and MAPE. As shown in Table 7, the MSE, RMSE, and MAPE values for model Equation 9 were lower, indicating that the MLR model with three input variables is superior. The regression analysis also revealed that CFA, CG, and CA, as concrete constituents, have a greater impact on the f_{cu} of concrete.

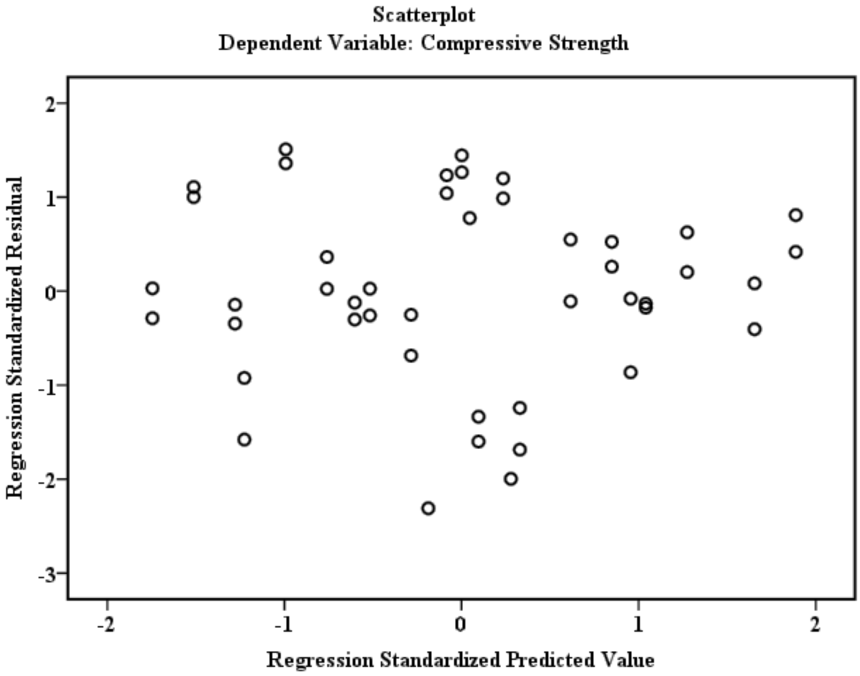

(a)

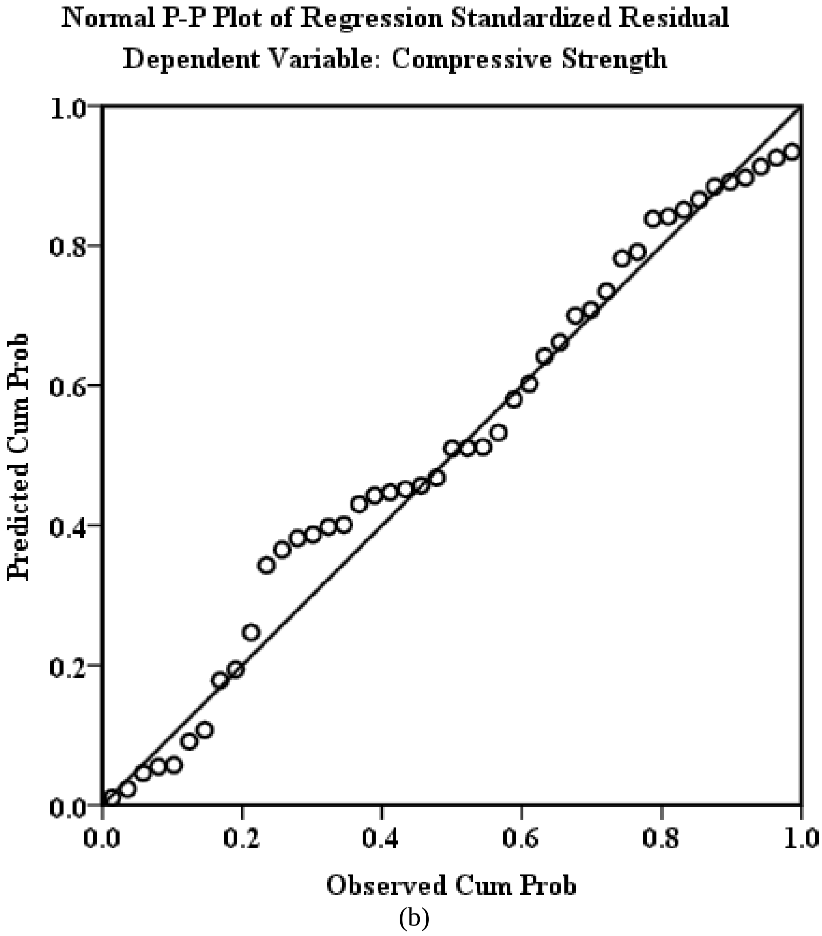

(b)

Fig. 5 - Residual plots (a) scatter plot of standardized regression residua; (b) standard P-P plot of regression standardized residual

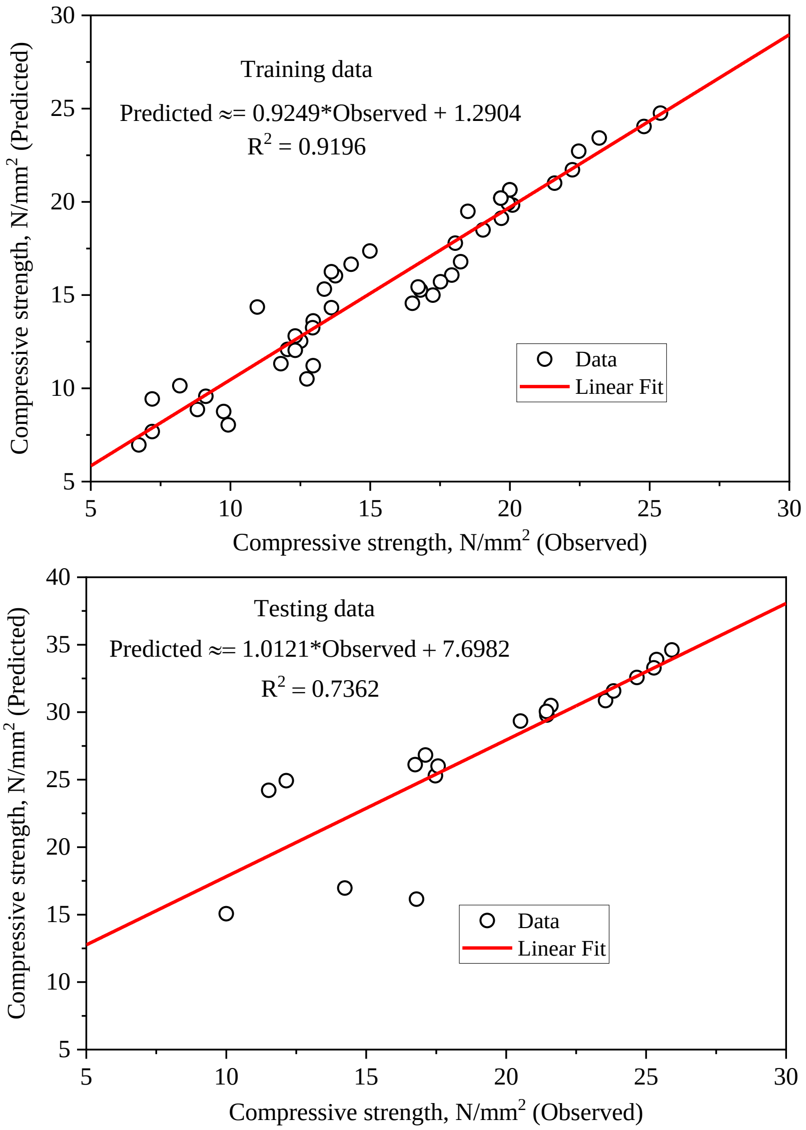

Fig. 6 - The scatter plots of observed and predicted values of f_{cu} for MLR Equation 8 model

3.3 Comparison between ANN and MLR Models

The regression analysis of the experimental (observed) data revealed that nearly two-thirds of the input variables (OPC, RHA, CFS, AS, and WB) did not contribute to the MLR's performance. This could be attributed to a nonlinear relationship or a very low correlation between these variables and f_{cu}. The chosen most likely ANN model, on the other hand, demonstrates a thorough understanding of the hidden relationships between these variables and the corresponding fcu. As a result, the increased ability of ANN to predict nonlinear behavior is noteworthy. The results of the performance indices of the developed MLR and ANN models, as shown in Table 7, show that ANN provides a more reliable estimate of compressive strength, f_{cu}, than MLR. The higher R^2 of 0.9972 and lower error estimates of ANN than those obtained by the MLR models supported previous studies conducted by Ni and Wang [37], demonstrating that ANN is a better predictive tool for solving concrete technology problems than traditional linear regression.

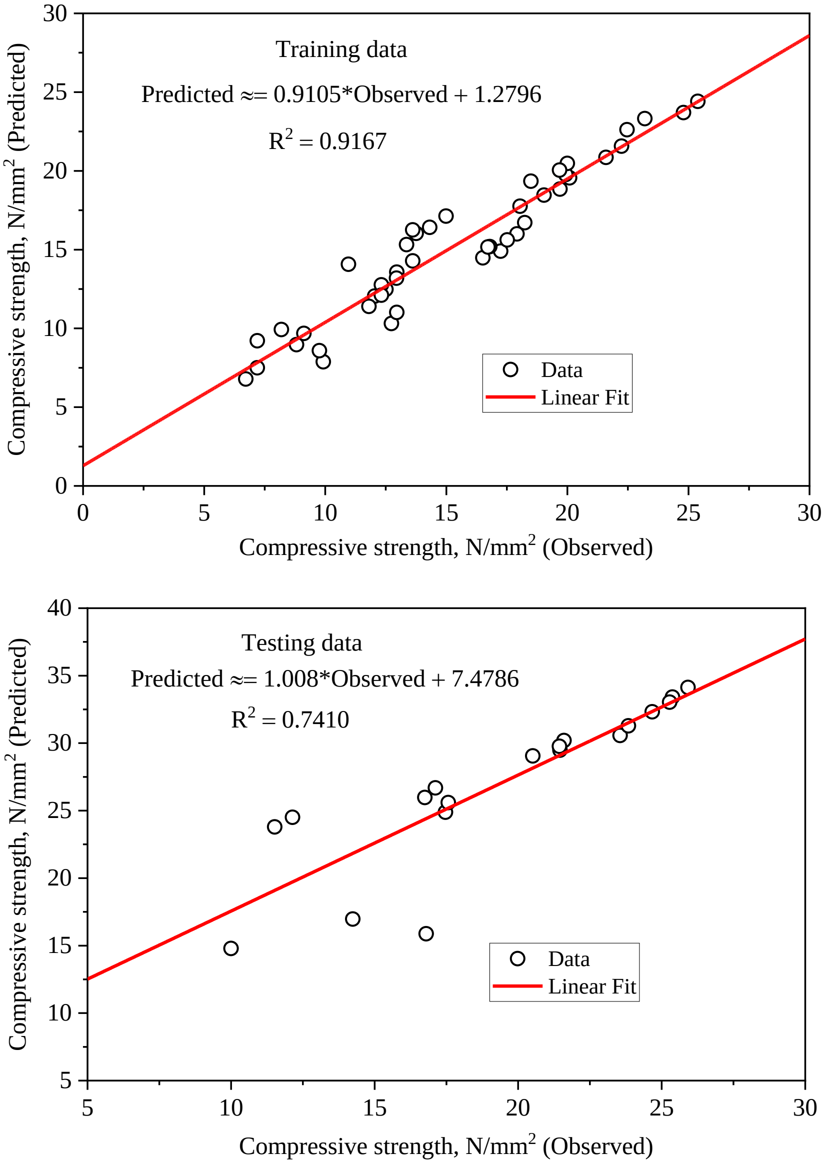

Fig. 7 - The scatter plots of observed and predicted values of f_{cu} for MLR Equation 9 model

Table 5 - Performance indices of the MLR model (Training)

MLR Equations	Training				
	R^2	*r*	MSE	RMSE	MAPE
8	0.9101	0.9540	1.9504	13.0834	15.2448
9	0.9167	0.9574	1.9702	13.2168	14.9806

Table 6 - Performance indices of the MLR model (Testing)

MLR Equations	Testing				
	R^2	*r*	MSE	RMSE	MAPE
8	0.7362	0.8580	71.5741	311.9841	413.5358
9	0.7410	0.8608	66.6308	290.4370	385.5221

Table 7 - Performance evaluation of MLR and ANN models

Model	Testing				
	R^2	r	MSE	RMSE	MAPE
MLR Equation 8	0.7362	0.8580	71.5741	311.9841	413.5358
MLR Equation 9	0.7410	0.8608	66.6308	290.4370	385.5221
ANN	0.9972	0.996	0.4177	1.8201	2.2935

4. Conclusions

This study reports the performance of the Artificial Neural Network, ANN, and the traditional Multiple Linear Regression, MLR in reproducing and predicting the f_{cu} of GPRC using a data set from the laboratory tests to obtain the appropriate value of compressive strength, f_{cu} of GPRC within a short time frame. Variable significant factors such as Ordinary Portland cement (OPC), Rice Husk Ash (RHA), Coal Fly Ash (CFA), Crushed granite (CG), Cupola Furnace Slag (CFS), Alkaline Solution (AS), Water-Binder Ratio (WB), and Concrete Age (CA) were used as input within the back-propagation ANN training process and backward elimination algorithm for MRL in the developed models. The MSE, RMSE, MAPE, and R^2 values were used to compare the observed and predicted compressive strength values. Based on satisfactory MSE, the most likely model architecture with eight input layers, thirteen hidden layers, and one output layer neurons was chosen after several trials. According to the MLR results, only three input variables, CFA, CG, and CA, are statistically significant with p-values less than 0.05. R^2 = 0.9972, MSE = 0.4177, RMSE = 1.8201, MAPE = 2.2935 for ANN and R^2 = 0.7410, MSE = 66.6308, RMSE = 290.4370, MAPE = 385.5221 for MLR. Furthermore, the developed ANN and MLR models can strongly predict the observed, tested f_{cu} of GPRC with minor discrepancies.

Furthermore, this implies a good fit between the ANN and MLR prediction models and the observed results. As a result, within the constraints of the concrete ingredients used, these models can predict the fcu of concrete. Based on the analysis and results, the following conclusions are reached: 1) the correlation and p-value results revealed that only three input variables (CFA, CG, and CA) are statistically significant in the development of the MLR model, and the others are reductants; 2) in the development of the ANN model, it was revealed that all (eight) input variables used were all significant; and 3) based on the statistical indices (R^2, MSE, etc.), ANN model shows to be the most reliable predictive model and has strong ability to predict nonlinear behavior when compared with MLR. Finally, the proposed ANNs and MLR methods provide a powerful tool to study the prediction of f_{cu} of concrete in a general situation.

Conflict of Interest

The authors received no direct funding for this research.

Acknowledgment

The authors wish to acknowledge the support of the University Research Committee (URC) and Faculty Research Committee (FRC) of the University of Johannesburg, South Africa.

References

[1] Afolayan, J. O., & Alabi, S. A. (2013). Investigation on the potentials of cupola furnace slag in concrete. International Journal Integrated Engineering, 5(2), 59-62.

[2] Arum, C., & Mark, G, O. (2014). Partial replacement of Portland cement by granulated cupola slag – sustainable option for concrete of low permeability. Civil and Environmental Research, 6(3), 17 – 26.

[3] Alabi, S. A., & Mahachi, J. (2020a). Behaviour of ground cupola furnace slag blended concrete at elevated temperature. Journal of Materials and Engineering Structure, 7:35-46.

[4] Reddy, B. S., Varaprasad, J., & Reddy, K. N. (2010). Strength and workability of low lime fly-ash based geopolymer concrete, India Journal Science and Technology, 3(12), 1188-1189.

[5] Shaikh, F. U. A. (2016). Mechanical and durability of fly ash geopolymer concrete containing recycled coarse aggregates. International Journal of Sustainable Built Environment, 5, 277–287.

[6] Bouaissi, A., Li, L. Y., Abdullah, M. M. A., & Bui, Q. B. (2019). Mechanical properties and microstructure analysis of FA-GGBS-HMNS based geopolymer concrete. Construction and Building Materials, 210, 198–209.

[7] Alabi, S. A., & Mahachi, J. (2020b). On the development of sustainable and strong concrete. Materials Today: Proceedings. https://doi.org/10.1016/j.matpr.2020.05.369.

[8] Alabi, S. A., & Mahachi J. (2020c). Chloride ion penetration performance of recycled concrete with different geopolymers. Materials Today: Proceedings. https://doi.org/10.1016/j.matpr.2020.04.199.

[9] Dash, M. K., Patro, S. K., & Rath, A. (2016). Sustainable use of industrial-waste as partial replacement of fine aggregate for preparation of concrete – a review. International Journal Sustainable Built Environment, 5, 484–

516.
[10] Thomas, C., Setién, J., & Polanco, J. A. (2016). Structural recycled aggregate concrete made with precast wastes. Construction Building Materials, 114, 536–546.
[11] Lau, T. L., Elleithy, W., Choong, W. K., Tze, T. Y., Lee, C. M,, & Modhwadia, A. L. (2014). Effects of recycled aggregates on concrete strengths. Materials Research Innovations, 18(6), 372-S6-374.
[12] De, L., Vieira, B. P., & de Figueiredo, A. D. (2016). Evaluation of concrete recycling system efficiency for ready-mix concrete plants. Waste Management, 56, 337–351.
[13] Butler, L. J., West, J. S., & Tighe, S. L. (2014). Towards the classification of recycled concrete aggregates: influence of fundamental aggregate properties on recycled concrete performance. Journal Sustainable Cement Based Materials, 3, 140–163.
[14] Mastali, M., Dalvand, A., & Sattarifard, A. (2016). The impact resistance and mechanical properties of reinforced self-compacting concrete with recycled glass fibre reinforced polymers. Journal of Cleaner Production, 124, 312-324.
[15] Khaloo, A., Raisi, E. M., Hosseini, P., & Tahsiri, H. (2014). Mechanical performance of self-compacting concrete reinforced with steel fibers. Construction and Building Materials, 51, 179-86.
[16] Kheder, G. F., & Al Jadiri, R. S. (2010). New Method for proportioning self-consolidating concrete based on compressive strength requirements. ACI Materials Journal, 107.
[17] Anuar, R., Ridzuan, A. R., & Ismail, S. (2011). Strength characteristic of geopolymer concrete containing recycled concrete aggregate, International Journal of Civil and Environmental Engineering, 11(1), 81-85.
[18] Ren, X., Zhang, L., Ramey, D., Waterman, B., & Ormsby, S. (2014). Utilization of aluminum sludge (AS) to enhance mine tailings-based geopolymer, Journal of Material Science, 1-12.
[19] Nath, P., & Sarker, P. K. (2104a). Use of OPC to improve setting and early strength properties of low calcium fly ash geopolymer concrete cured at room temperature. Cement and Concrete Composites, 1-33
[20] Nath, P., & Sarker, P. K. (2014b). Effect of GGBFS on setting, workability and early strength properties of fly ash geopolymer concrete cured in ambient condition. Construction and Building Materials, 66, 163–171
[21] Torres-Carrasco, M., & Puertas, F. (2105). Waste glass in the geopolymer preparation: mechanical and microstructural characterization. Journal of Cleaner Production, 2015; 1-34.
[22] Tho-In T, Sata V, Boonserm K, Chindaprasirt P, (2017). Compressive strength and microstructure analysis of geopolymer paste using waste glass powder and fly ash. Journal of Cleaner Production, 2017; 1-30.
[23] Shalika, S., & Hemant, S. (2016). Abrasion resistance of geopolymer concrete at varying temperature. Journal of Mechanical and Civil Engineering, 13(1):22-25.
[24] Sultana, M. E., Abo-El-Eneinb, S. A., Sayeda, A. Z., EL-Sokkaryc, T. M., & Hammada, H. A. (2018). Incorporation of cement bypass flue dust in fly ash and blast furnace slag-based geopolymer. Case Studies in Construction Materials, 8, 315–322.
[25] Sadrmomtazi, J., Sobhani, M. A., & Mirgozar. (2013). Modeling compressive strength of EPS lightweight concrete using regression, neural network and ANFIS. Construction and Building Materials, 42, 205–216.
[26] Bal, L., & Buyle-Bodin, F. (2013). Artificial neural network for predicting drying shrinkage of concrete. Construction and Building Materials, 38, 248–254.
[27] Parichatprecha, R., & Nimityongskul, P. (2009). Analysis of durability of high performance concrete using artificial neural networks. Construction and Building Materials, 23, 910–917.
[28] Shafabakhsh, G. H., Jafari, Ani O, & Talebsafa, M. (2015). Artificial neural network modeling (ANN) for predicting rutting performance of nano-modified hot-mix asphalt mixtures containing steel slag aggregates. Construction and Building Materials, 85, 136–143.
[29] Fatih, O., Cengiz, D. A., Okan, K., Erdal, U., & Harun, T. (2009). Comparison of artificial neural network and fuzzy logic models for prediction of long-term compressive strength of silica fume concrete, Advances in Engineering Software, 40, 856–863.
[30] Garzon-Roca, J., Marco, C. O., & Adam, J. M. (2013). Compressive strength of masonry made of clay bricks and cement mortar: Estimation based on Neural Networks and Fuzzy Logic, Engineering Structures, 48, 21–27.
[31] Topc, I. B., & Sarıdemir, M. (2008). Prediction of compressive strength of concrete containing fly ash using artificial neural networks and fuzzy logic. Computational Materials Science, 41, 305–311.
[32] Oztas, A., Pala, M., Ozbay, E., Kanca, E., Naci, C., Aglar, M., & Bhatti, A. (2006). Predicting the compressive strength and slump of high strength concrete using neural network. Construction and Building Materials, 20, 769–775.
[33] Pala, M., Ozbay, E., Oztas, A., & Ishak Yuce, M. (2007). Appraisal of long-term effects of fly ash and silica fume on compressive strength of concrete by neural networks. Construction and Building Materials, 21, 384–394.
[34] Lee, S. C. (2003). Prediction of concrete strength using artificial neural networks. Engineering Structures, 25, 849–857.
[35] Hodhod, O. A., & Ahmed, H. I. (2014) Modeling the corrosion initiation time of slag concrete using the artificial neural network. Housing and Building National Research Center Journal, 1-4.
[36] Alshihri, M. M., Azmy, A. M., & El-Bisy, M. S. (2009). Neural networks for predicting compressive strength of

structural light weight concrete. Construction and Building Materials, 2009; 23:2214–2219.
[37] Ni, H. G., & Wang, J. Z. (2000). Prediction of compressive strength of concrete by neural networks. Cement and Concrete Research, 30, 1245-1250.
[38] Bilim C, Atis CD, Tanyildizi H, Karahan O. (2009). Predicting the compressive strength of ground granulated blast furnace slag concrete using artificial neural network. Advances in Engineering Software, 40, 334–340.
[39] Sarıdemir, M. (2009). Predicting the compressive strength of mortars containing metakaolin by artificial neural networks and fuzzy logic. Advances in Engineering Software, 40, 920–927.
[40] Duan, Z. H., Kou, S. C., & Poon, C. S. (2013). Prediction of compressive strength of recycled aggregate concrete using artificial neural networks, Construction and Building Materials, 40, 1200–1206.
[41] Khademi, F., Akbari, M., Jamal, S. M., & Nikoo, M. (2017). Multiple linear regression, artificial neural network, and fuzzy logic prediction of 28 days compressive strength of concrete, Frontiers of Structural and Civil Engineering, 11(1), 90–99.
[42] Sobhani, J., Najimi, M., Pourkhorshidi, A. R., & Parhizkar, T. (2010). Prediction of the compressive strength of no-slump concrete: A comparative study of regression, neural network and ANFIS models. Construction and Building Materials, 24, 709–718.
[43] Ul-Saufie, A. Z., Yahya, A. S., & Ramli, N. A. (2011). Improving multiple linear regression model using principal component analysis for predicting PM10 concentration in Seberang Prai, Pulau Pinang. International Journal of Environmental Sciences, 2(2), 415-422.
[44] BS 12 (1995). Specification for Portland cement. British Standard Institution, London, United Kingdom.
[45] ASTM 1602 (2012). Standard Specification for mixing water used in the production of hydraulic cement concrete. ASTM International, West Conshohocken, PA.
[46] Lee, S. (2003). Prediction of concrete strength using artificial neural networks. Engineering Structures, 25, 849–857.
[47] Shabani, A., & Norouzi, M. (2015). Predicting cation exchange capacity by Artificial Neural Network and Multiple Linear Regression using terrain and soil characteristics. Indian Journal of Science and Technology, 8(28), 1-10.
[48] Zurada, J. (1992). Introduction to artificial neural systems. Info Access Distribution Ltd.
[49] Tanyildizi, H., Özcan, F., Atis, C. D., Karahan, O., & Uncuog, E. (2009). Comparison of artificial neural network and fuzzy logic models for prediction of long-term compressive strength of silica fume concrete. Advanced Engineering Software, 40, 856–863.
[50] Chen, L. (2010). Grey and neural network prediction of concrete compressive strength using physical properties of electric arc furnace oxidizing slag. Journal of Environment Engineering and Management, 20(3), 189–194.
[51] Garzón-roca, J., Marco, C. O., & Adam, J. M. (2013). Compressive strength of masonry made of clay bricks and cement mortar: estimation based on neural networks and Fuzzy Logic. Engineering Structures, 48, 21–27.
[52] Shmueli, G. (2010). To explain or to predict?. Statistical Science, 25(3), 289-310.
[53] Masters T. Practical neural network recipes C++. San Diego, California: Academic Press; 1993.